Short Communication: The trouble with time to steady state calculated from computational landscape evolution models

Nicole M. Gasparini[1], Adam M. Forte[2], and Katherine R. Barnhart[3,4,5]

[1]Tulane University, Earth and Environmental Sciences Department, New Orleans, LA, USA
[2]Department of Geology & Geophysics, Louisiana State University, Baton Rouge, LA, USA
[3]University of Colorado at Boulder, Cooperative Institute for Research in Environmental Sciences, Boulder, CO, USA
[4]University of Colorado at Boulder, Department of Geological Sciences, Boulder, CO, USA
[5]Now at U.S. Geological Survey, Geologic Hazards Science Center, Golden, CO, USA

Correspondence: Nicole Gasparini (ngaspari@tulane.edu)

Abstract.

Quantifying the timescales over which landscapes evolve is critical for understanding past and future environmental change. Computational landscape evolution models are one tool among many that have been used in this pursuit. We compare numerically modeled times to reach steady state for a landscape adjusting to an increase in rock uplift rate. We use three different numerical modeling libraries and explore the impact of time step, grid type, numerical method for solving the erosion equation, and metric for quantifying time to steady state. We find that modeled time to steady state is impacted by all of these variables. The sensitivity of time to steady state to computational time step is not consistent among models or even within a single model. In some cases, drainage rearrangement extends the time to reach steady state, but this is not consistent in all models or grid types. The two sets of experiments operating on voronoi grids have the most consistent times to steady state when comparing across time step and metrics. On a raster grid, if we force the drainage network to remain stable, time to steady state varies much less with computational time step. In all cases we find that modeled time to steady state is longer than that predicted by an analytical equation. Our results show that the predicted time to steady state from a numerical model is, in many cases, more reflective of drainage rearrangement than the time for an uplift wave to propagate through a fixed drainage network.

1 Introduction

The concepts of steady-state landscapes and characteristic timescales for landscapes to transition from one steady state to another, i.e., response times, have been widely used as framework for interpreting landforms and landscape evolution (e.g., Whipple, 2001; Whipple and Meade, 2004; Hilley et al., 2004; Stolar et al., 2006; Whipple and Meade, 2006; Roe et al., 2008; Forzoni et al., 2014; Goren, 2016; Armitage et al., 2018), and what signals may be preserved in the sedimentary record (e.g., Castelltort and Van Den Driessche, 2003; Simpson and Castelltort, 2012; Romans et al., 2016; Li et al., 2018; Straub et al., 2020; Tofelde et al., 2021). If landscapes evolve to a predictable steady form that is a function of environmental drivers, presumably we could invert landscape form to infer these environmental drivers (e.g., Snyder et al., 2000; Densmore, 2004; Kirby and Whipple, 2012; Whittaker, 2012; Hurst et al., 2019; Adams et al., 2020). Further, steady-state morphology is a well-

established way to compare modeled landscapes (e.g., Tucker and Bras, 1998; Tucker and Whipple, 2002; Gasparini et al., 2004; Anders et al., 2008; Roering, 2008; Han et al., 2015; Shobe et al., 2018; Campforts et al., 2022).

While steady state can be used to imply a variety of different conditions, here we specifically consider topographic steady state (e.g., Willett and Brandon, 2002). To determine whether a landscape has reached topographic steady state, we need to know how to measure it (either in the field or in a simulation). There are many options for how to measure topographic steady state in a computational model, and accordingly, an initial question is which steady-state metric in a numerical model is most reliable. If we measure steady state using erosion rates or sediment fluxes, over what time scales should these fluxes be measured? Further, how much variability in sediment flux can we expect under steady conditions? If steady state is measured using landscape metrics, such as total relief, which metrics are used? Similarly, how much variability in these metrics is acceptable while still maintaining at steady state?

Once a criterion for steady state is established, a computational model can be used to measure the time it takes for a landscape to reach steady state following a perturbation. Given an understanding of time-to-steady-state, many different inferences may be drawn with implications for the interpretation of specific landscapes on Earth or other planets. If a particular configuration of initial and boundary conditions results in landscapes that reach steady state relatively quickly (in comparison with variations in environmental forcings), then we can expect similarly configured real landscapes to reach steady state. However, if landscapes take so long to adjust that environmental changes happen more frequently, we might expect to rarely observe steady-state landscapes. Similarly, if we can establish that response times of simulated landscapes to perturbations behave systematically and predictably as a function of the environmental drivers, then simulated response times could theoretically be used to establish characteristic time scales for processes (e.g., Whipple et al., 2017; Lyons et al., 2020). Further, if time scales of landscape evolution and/or natural forcings are known in study landscapes, models could be used to test competing landscape evolution scenarios, interpret processes controlling landscape evolution, and establish the impact of competing timescales on landscape form (e.g., Densmore et al., 2007; Attal et al., 2008; Godard et al., 2013; Whittaker and Boulton, 2012; Mackey et al., 2014; Brocard et al., 2016). Establishing the reliability of time to steady state derived from landscape evolution models is thus a consequence of this metric's importance for interpreting landscape evolution models and connecting inferences drawn from them with datasets collected on Earth.

In this short communication we show how time to steady state changes in otherwise identical computationally modeled landscapes. We quantify steady state in different models that use different numerical methods and grid types. In all of our model scenarios we evaluate four different metrics for quantifying steady state. We show that flow routing methodology is the biggest control on time to steady state in our modeling experiments, but that the impact of flow routing on drainage reorganization also varies with grid type. Similarly, computational time step and method for quantifying steady state also impact the time to steady state. In other words, we find time to steady state from numerical models to be inconsistent, and, in some cases, of minimal use when interpreting real landscapes, especially when considering the outcome of a single or very small set of landscape simulations.

2 Modeling environments

The three modeling environments used in this paper were chosen because the authors have experience using them. The choice of these models says nothing about the value of these modeling environments or the variety of other modeling environments that exist. We do not assume that these models represent the behavior of all modeling environments. That said, these three modeling environments allow us to explore the sensitivity of time to steady state to multiple grid types and numerical methods.

2.1 CHILD

The CHILD modelling environment was developed in the late 1990s (e.g., Tucker et al., 1999, 2001a, b). It operates on a triangular irregular network, forming a voronoi diagram, here referred to as a voronoi grid for consistency with the other grid types. CHILD uses an explicit finite difference solution of the stream power process equation.

CHILD is a C++ code that is open source and available through GitHub (https://github.com/childmodel/child; accessed 08 September 2022). Although CHILD is no longer actively in development, it was widely used in the past 20 years and continues to be used at the time of writing. Because of its familiarity to the authors, its application on a voronoi grid, and its advanced stage of development, we used it in this study.

2.2 Landlab

Landlab is Python library for modeling surface processes on regular and irregular grids (Hobley et al., 2017; Barnhart et al., 2020). In this study we implement computer models that use raster, hexagonal, and voronoi grids. (Landlab also supports radial grids but these are not tested in this study.) Landlab is open source and available through GitHub (https://github.com/landlab/landlab; accessed October 14, 2022). This study used Landlab version 2.4.2.dev0. Landlab is in active development and is currently maintained through CSDMS (Tucker et al., 2022). The stream power process component used in all Landlab computer models in this study implements a version of the Fastscape implicit finite difference numerical algorithm (Braun and Willett, 2013). The Fastscape numerical algorithm was designed to be more stable than most finite difference methods (Braun and Willett, 2013).

2.3 TTLEM

TTLEM is part of the TopoToolbox Matlab library. Many readers may be familiar with the DEM (digital elevation model) analysis tools that are contained within TopoToolbox (e.g., Schwanghart and Scherler, 2014). TTLEM is an LEM that is distributed with these tools and uses the TopoToolbox library for many of the core functions within the LEM, e.g., flow routing (Campforts et al., 2017) (Available at https://github.com/wschwanghart/topotoolbox; accessed December 7, 2022).

TTLEM contains three numerical algorithms for solving the stream power equation on a raster grid. In this study we use TTLEM computer models that implement the Fastscape implicit numerical algorithm, an explicit finite difference algorithm, and the total variation diminishing finite volume method (TVD_FVM). TVD_FVM is designed to be highly accurate and limit numerical diffusion (Campforts and Govers, 2015).

2.4 LEMs and comparison rational

Using the three modeling environments described above, we created seven different LEMs which we use to calculate time to steady state. These different LEMs are described in Table 1. These three modeling environments allow us to compare how grid type and the numerical method for solving the stream power equation impact time to steady state.

LEM	Modeling Environment	Grid Type	Numerical Method
CVE	CHILD	voronoi	explicit
LVI	Landlab	voronoi	fastscape (implicit)
LHI	Landlab	hexagonal	fastscape (implicit)
LRI	Landlab	raster	fastscape (implicit)
TRI	TTLEM	raster	fastscape (implicit)
TRT	TTLEM	raster	TVD_FVM
TRE	TTLEM	raster	explicit

Table 1. Table of different LEMs used in this study. We use the LEM abbreviated names in column 1 to refer to the different model scenarios. The first letter in the abbreviated name stands for the modeling environment: C for CHILD; L for Landlab; and T for TTLEM. The second letter stands for the grid type: V for voronoi; H for hexagonal; and R for raster. The third letter stands for the numerical method used to solve the stream power equation: E for explicit; I for implicit; T for TVD_FVM.

3 Stream power equation

All of the model environments we consider use the stream power equation to represent the evolution of fluvial profiles. We only consider fluvial erosion in our LEMs. Erosion is sustained throughout all simulations by uniform, steady rock uplift. The equation controlling the change in topographic elevation at each node is,

$$\frac{dz}{dt} = U - KA^m S^n \tag{1}$$

where z is node elevation; t is time, and dt is the computational time step; U is the rock uplift rate; K is the erodibility parameter; A is the drainage area at a node; S is the topographic slope (negative of the spatial derivative in elevation, assuming directionality is in the downslope direction) at a node; and m and n are positive exponents. Note that the second set of terms on the right-hand-side of equation 1 is the widely used stream power equation (SPE) that describes detachment limited fluvial incision,

$$E = KA^m S^n \tag{2}$$

where E is fluvial incision. Derivations, dynamics, and limitations of the SPE have been described in detail in numerous publications and we refer interested readers to such sources (e.g., Howard, 1994; Whipple and Tucker, 1999; Lague, 2014).

4 Experimental set-up

Each of our numerical experiments quantified the time it takes for a low rock uplift rate, steady-state landscape to fully adjust to an increase in rock uplift rate using a specific LEM scenario (Table 1), initial condition, and a range of computational timesteps. We did not formally quantify that the initial low uplift landscapes were at steady state. Instead we generated initial conditions with simulations that ran for 100 million years. As will be apparent from our results, this is more than enough time for our landscapes to reach steady state regardless of chosen metric or threshold for identifying steady state. In some cases we stopped the initial runs before 100 million years because the landscape became perfectly static. This experimental design, in which an initially steady landscape is perturbed by changing the uplift rate, is similar to previous modeling studies (e.g., Rosenbloom and Anderson, 1994; Whipple and Tucker, 1999, 2002; Gasparini et al., 2007; Attal et al., 2011), which is why we chose it.

As described below, we kept as much constant among the simulations with different LEMs as possible. However, we did not do anything to change the models from "off the shelf". In other words, we used the modeling environments without changing any of the internal code that implements the numerical algorithms. Where appropriate, we did change parameters within the different modelling environments to try to assure that their behavior was as comparable as possible. For example, all the raster models use D8 flow routing (Tarboton, 1997), and this was an option that we chose when using the LRI model to make it more similar to the TRI model. In contrast, there are multiple ways to calculate a topographic gradient at a grid cell in a computational model. Choosing the algorithm used to make this calculation is not exposed to the user for these models, and accordingly we can not ensure that each model calculates topographic gradient in the same way.

The simulations that created the initial steady state landscape were started from a surface with elevation values randomly chosen between 0.0 and 1.0 meters. The random elevation initial surface was used because it creates more realistic looking drainage networks. The raster grids had 200 by 200 nodes, and the spacing between nodes in the x and y direction was 100 meters. All the simulations using a raster grid in different models used the same exact initial topographic surface (LRI, TRI, TRT, and TRE). The simulations that use a voronoi grid had an average node spacing of 100 m, but the spacing varied (in a regular way) to define the grid. The initial condition was a similar noisy surface as used with the raster grids, and the same exact initial surface was used in the CVE and LVI simulations. Regardless of the type of grid, all the grids were $\approx$ 20 km by $\approx$ 20 km with $\approx$ 100 m resolution.

The boundary conditions used in all simulations were the same. All of the nodes on the perimeter of grid were open boundaries where water can exit, but not enter, the grid. The elevation of the perimeter boundary nodes was fixed at zero meters and did not change during the simulations. In other words, the perimeter nodes were not uplifted but the rest of the grid was uplifted. U and K were spatially uniform and set at 1e-4 m/yr and 5e-6 yr^{-1}, respectively, in all the initial simulations. m and n were also spatially uniform and set at 0.5 and 1, respectively.

We explored how the time step value, dt in equation 1, impacts the time to steady state. Each model should be stable, and produce the correct analytical solution, when the time step satisfies the Courant–Friedrichs–Lewy condition:

$$C_{max} > \frac{vdt}{dx} \tag{3}$$

where C_{max} is the Courant number, ≈ 1.0 in stable conditions; v is the speed that an erosional wave will move through the network, and dx is the spacing between nodes. When using the stream power process equation with $n = 1$, v is approximated as

$$v \approx KA^m. \tag{4}$$

To calculate the maximum time step for a stable Courant condition (dt, equation 3), we needed to know the largest drainage area in the modeled network to estimate the fastest wave speed (equation 4). Because we started with a noisy surface and drainages evolved out of the noise, the area of the largest watershed was unknown until the landscape reached steady state. However, we had to choose a stable dt before the landscape evolved. Therefore we estimated the size of the largest drainage. We assumed the maximum drainage area will be one-fourth of the total area of the grid, or 49 km^2. This value was intended as an overestimation, ensuring that we calculated a stable time step with Eqs. 3 and 4.

We combined equations 4 and 3 to calculate a value of dt. For the values chosen for K and m, $C_{max} = 1$, and our estimated value for the maximum drainage area, we calculated a stable dt of 2857 years. We then chose dt =2,500 yrs as the base-case model time step because it should result in stable simulations. We explored how landscape response time changed by changing dt. We ran four simulations with each model, reducing dt to 250 yrs and increasing dt to 25,000 and 100,000 yrs, or approximately 10 and 40 times greater than the stable condition, respectively.

The decision to use time steps longer than the estimated stable time step is motivated by the results shown in (Braun and Willett, 2013). They state that their numerical algorithm, which is the implicit numerical method used in TRI and all Landlab models, is accurate even when the time step is more than 100 times the stable condition. The stability of the algorithm is also discussed in (Braun and Deal, 2023). However, simulations from models employing either the explicit finite difference or TVD_FVM algorithms did not produce accurate, or even sensible results, with time steps longer than the predicated stable value. Hence results with all times steps are only shown from models using the implicit solution. In one case, TRI, we also performed two extra simulations with dt = 1,000 and 10,000 yrs. This was done based on preliminary results to fully explore sensitivity of time to steady state to dt.

We use the steady initial conditions produced from each model simulation and time step combination as the initial condition for the corresponding transient simulations. We increase rock uplift rate uniformly across the grid by a factor of five, to U=5e-4 m/yr. As the landscape evolves in response to the new, higher uplift rate, we track the steady-state metrics to quantify differences in time to steady state.

In all of our initial simulations we re-calculated flow directionality at every time step. However, after running the simulations we observed that in some cases the drainage network rearranged, and we wanted to explore how this affects time to steady state. Thus, we performed two more numerical experiments using TTLEM with the three different numerical methods (TRI, TRE, TRT). First, we re-ran all of the TTLEM empirical models but did not reroute flow at every time step during the transient simulations. In other words, we forced the network to remain static during the adjustment to a higher uplift rate. Second, we generated new steady-state initial conditions and used them for another set of uplift increase experiments. For these simulations, we started with a different initial white noise grid to create the low uplift steady state topography. Because the initial white noise

determines the network details, these landscapes have a different network despite being run with the same model, parameters, and boundary conditions.

5 Time to steady state

Here we describe the metrics we use to empirically quantify time to steady state. We also describe the analytical equation previously presented by Whipple and Tucker (1999) and Whipple (2001) that we use to predict time to steady state. In the results section we will compare the empirically derived steady-state times with the analytically predicted values.

5.1 Numerically modeled

Theoretically steady state is reached when equation 1 is equal to zero, or when rock uplift rate U and fluvial incision rate E are equal at every node. Although steady state is often used and referred to in numerical modeling studies, the criteria for reaching steady state, or determining when $E = U$ everywhere on the grid, is not always explicitly described. Here we test four metrics for determining when steady state is reached. We refer to these collectively as the steady-state metrics.

The temporal change in maximum elevation, Δz^t_{max} was calculated as,

$$\Delta z^t_{max} = |max\left(z^t_i\right) - max\left(z_i^{t-100{,}000}\right)|, \tag{5}$$

where $max\left(z^t_i\right)$ is the maximum grid elevation within the domain at time t; and $max\left(z_i^{t-100{,}000}\right)$ is the maximum grid elevation within the domain at time $t - 100{,}000$.

The temporal change in mean elevation, Δz^t_{mean} was calculated as,

$$\Delta z^t_{mean} = |mean\left(z^t_i\right) - mean\left(z_i^{t-100{,}000}\right)|, \tag{6}$$

where $mean\left(z^t_i\right)$ is the mean grid elevation within the domain at time t; and $mean\left(z_i^{t-100{,}000}\right)$ is the mean grid elevation within the domain at time $t - 100{,}000$.

The temporal change in maximum local elevation, $\Delta z^t_{max(loc)}$ was calculated as,

$$\Delta z^t_{max(loc)} = max\left(|z^t_i - z_i^{t-100{,}000}|\right). \tag{7}$$

The difference between equations 5 and 7 is that the former finds the difference between the maximum elevation of the entire domain at two different times, whereas the latter finds the difference in elevation at every node in the landscape between two different time steps and uses the maximum of those differences. The units on all of the elevation change metrics are meters.

Finally, the temporal change in sediment flux, ΔQs^t, was calculated as,

$$\Delta Qs^t = \sum Qs^t_i - \sum Qs_i^{t-100{,}000}, \tag{8}$$

where $\sum Qs^t_i$ is the summation of the erosion rate at every node on the landscape at time t; and $\sum Qs_i^{t-100{,}000}$ is the summation of the erosion rate at every node on the landscape at time $t - 100{,}000$. The models do not track the sediment flux explicitly

when using the SPE, which is why we use the local erosion rate as a proxy for sediment flux. In all of the grids the cell size is nearly uniform, hence the summation of erosion rate is a good proxy for the sediment flux. The units of ΔQs are meters per year.

In all cases the steady-state metrics are calculated over a temporal difference 100,000 yrs, which was set by the longest time step of the simulations being compared. This was done to ensure equivalent comparisons between the simulations as some degree of differences in time to steady state would be expected if we calculated these metrics over different time intervals between simulations. The first time that the topographic metrics were calculated is at 100,000 yrs into the simulation. With the sediment flux metric, the first calculation is done at 200,000 yrs, because there is no sediment flux at time zero in the simulation.

As a landscape evolves towards steady state, all of the steady-state metrics should approach zero. When exactly a new steady state is reached could be defined as when the metric value passes below a predetermined threshold. The strictest definition would be when a metric reaches zero. We note that differences in the accuracy of calculations in different modeling environments could lead to some of the metrics never reaching zero. Also, the time at which a particular metric appears to reach zero will depend on the floating point precision of the programming environment in which the metric is calculated. One could also use the rate of change in the value of a steady-state metric as a criteria for reaching steady state.

Here we define the time to steady state to be 10^{-5} meters for the elevation metrics or 10^{-6} meters per year for the flux metric. This may seem conservative. For example, this means the maximum elevation in a landscape changes by less than 10^{-5} meters over 100,000 years. We chose that threshold after seeing the results, as we did not know exactly what to expect in advance. However, the choice of the threshold value makes sense in light of the behavior of these metrics, as will be illustrated below.

5.2 Analytical equation

Following Whipple and Tucker (1999), Whipple (2001) showed that the predicted time to steady state following an increase in rock uplift in a landscape evolving according to equation 1 and with $n = 1$ is

$$T_A = \frac{\beta}{K} \tag{9}$$

where

$$\beta = k_a^{-\frac{m}{n}} \left(1 - \frac{hm}{n}\right)^{-1} \left(L^{1-\frac{hm}{n}} - x_c^{1-\frac{hm}{n}}\right). \tag{10}$$

In equation 9, T_A is the analytical time to steady state, K is the erodibility in equation 2. In equation 10, x_c is hillslope length, and m and n are the exponents in equation 2. Equation 10 also requires empirical parameters k_a and h from the equation developed by Hack (1957):

$$A = k_a x^h \tag{11}$$

where x is distance from the divide and A is drainage area. Note that equation 10 only holds when $\frac{hm}{n} \neq 1$ which is the case in all of our experiments.

We use data from the largest watershed in the modeled landscapes to calculate k_a and h. In simulations in which there is drainage rearrangement, and hence slight changes in these parameters while the simulation approaches a steady state, we use values at the end of the simulation time, which was 50 million years for the majority of our simulations. As none of our simulations formally included hillslopes, i.e., we do not consider diffusion and the diffusion constant was set to 0 in our simulations, we set x_c in equation 10 to 0.

6 Time to steady state results

Time series of all our metrics in all of our numerical experiments are illustrated in figure 1. Each column of figure 1 shows the time series of one of the four steady-state metrics. The different lines in each plot are the results using different computational time steps.

The top two rows of figure 1 illustrate the results for TRI and LRI LEMs, which have the same grid type and use the same numerical method to solve equation 1. Using our threshold values (10^{-5} m for topographic metrics and 10^{-6} m/yr for the flux metric) to reach steady state, the estimated time to steady state varies by tens of millions of years for the same model environment and steady state metric, depending on the time step. There is no consistent trend between time to steady state and time step. That is, time to steady state does not always increase or decrease with increasing time step. When comparing the steady-state elevation metrics among the TRI simulations, the time to steady state can increase by over 30 million years between the fastest and slowest modeled times to steady state. When comparing between the two model environments but with the same time step and steady state metric, the predicted time to steady state can vary by more than 20 million years.

In contrast, if one were to use the time at which a metric levels off and oscillates around a value, the estimated times to steady state would be closer for a given metric. This is regardless of the time step or the LEM in the simulations with a raster grid. However, the value that a given metric levels off at differs with time step in some cases (e.g. change in maximum elevation for the LRI model). Also, it is not a smooth asymptotic approach, as one might expect from these simulations. Notably, variation in the change in maximum local elevation stays fairly steady at a value between 10 and 100 m for the entire simulation, until the landscape stabilizes and the value continually decreases. In other words, with the change in maximum local elevation, there is no initial decrease in the metric and then a stabilization, as occurs with the change in mean elevation and flux metrics.

The steady-state metrics from the TRT and TRE simulations (third and fourth rows of figure 1) showed similar behavior as discussed above for the TRI and LRI simulations. The numerical methods used with TRT and TRE are not stable with larger time steps. Thus, the impact of time step on the steady-state metric values was not as large, given we only illustrate results using three stable time steps. However, the shortest time step does result in the longest time to steady state for both TRT and TRE, regardless of the metric. In all cases TRT and TRE predict shorter times to steady state for a given time step and metric than the TRI models predict.

The Landlab models using the hexagonal and voronoi grids (LVI and LHI, fifth and sixth rows of figure 1) all reach steady state at shorter times than the LRI simulations, for a given time step and steady state metric. Further, the LVI and LHI simulations have less of a range in predicted steady state time as a function of dt when comparing with the LRI simulations.

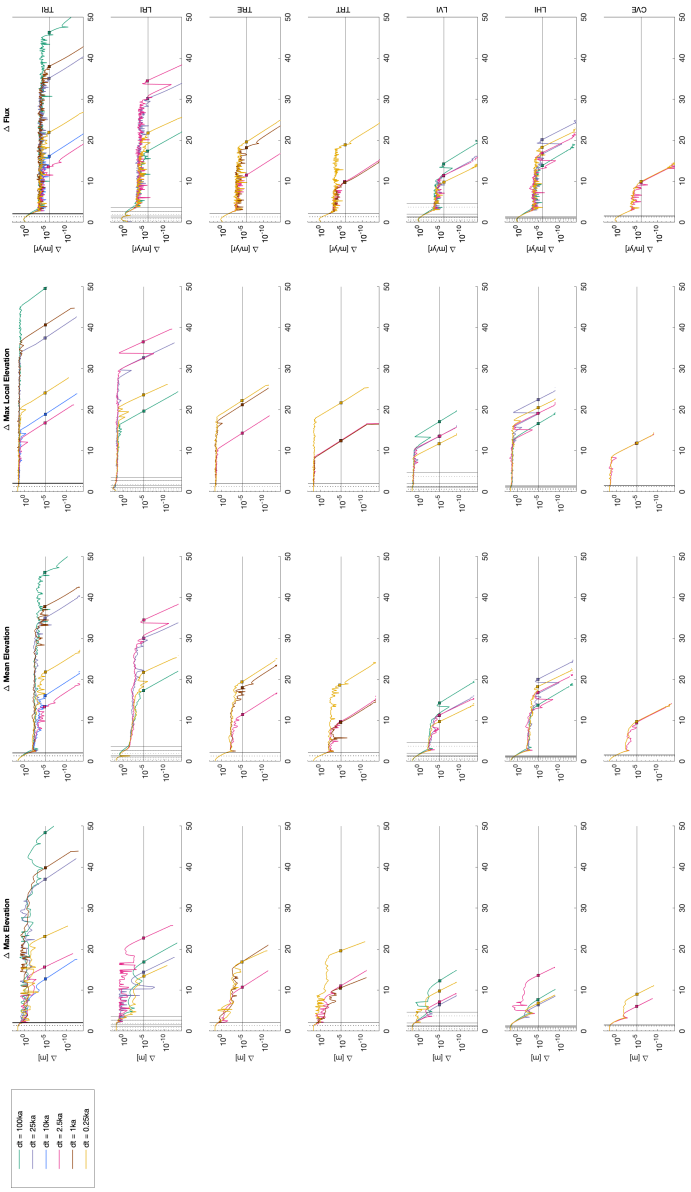

Figure 1. Time series of four different steady-state metrics, in columns, that can be used for evaluating when a landscape has reached steady state. Each row has the results from a different LEM (Table 1). The vertical lines are the analytical response times using the mean stream length (dashed) or longest stream length (solid). The x axis is time in millions of years in all the plots. Note that the extent of the x and y axes is the same in all the subplots.

These results are summarized in Figure 2 which compares the ratio of the modeled time to steady state using the metric threshold value T_E with the analytically predicted time to steady state (9), T_A. In theory, this should normalize the response times by expected differences related to either channel length or differences in length to drainage area scaling. One constant among all the simulations is that the empirical time to steady state is greater than the analytically predicted value. In other words, $\frac{T_E}{T_A} > 1$ always. This holds true regardless of time step or steady-state metric. The models using a voronoi grid (LVI and CVE) consistently have the smallest values of $\frac{T_E}{T_A}$; these are the only two models that, regardless of the metric or time step, $\frac{T_E}{T_A} < 10$ always. Note that LVI and CVE use different numerical methods for solving the stream power equation.

For some combinations of steady-state metrics and specific simulations, it would be possible to choose thresholds for the respective metric that would approximately equal the analytical time to steady state T_A, but not consistently. For example, the $\Delta z^t_{max(loc)}$ metric has limited change until well beyond T_A for most simulations and thus it would be challenging to choose a threshold that would result in a T_E value near T_A. For the other metrics, though, it would be generally possible to choose a threshold such that $T_E \approx T_A$. We emphasize that these threshold values would largely be different depending on the particular simulation, would not be known until after the experiments had been run, and that the continued variation in these metrics beyond T_A imply that some amount of measurable landscape change persists beyond the predicted analytical response time.

Before doing the computational experiments, we had hypothesized that the empirical steady state would vary monotonically with time step, in part because this is implied by results of Braun and Willett (2013), e.g., their figure 4, exploring the dynamics of the implicit solution to the stream power equation. The lack of relationship between empirical steady state and time step is especially noticeable in the TRI simulations, which we ran with six time steps. We wanted to rule out that this lack of relationship was not because of an initial landscape and network that, just by chance, led to odd results. Thus, we reran all of the TTLEM simulations on different steady-state landscapes that were produced using the same process as the first set of simulations, just with a different initial random surface. In these ALT-TTLEM simulations, there is again no relationship between time to steady state and time step (second row of figure 2). Further, these results do not match the patterns in the first set of TTLEM simulations. For example, comparing the TRT simulations, in our first set of simulations, the smallest time step produced the longest times to steady state, regardless of metric. Contrasting that with the ALT-TRT simulations, the smallest time step produced the shortest times to steady state, regardless of the metric.

When comparing the evolving topographies, we observed that the CVE simulations have no drainage rearrangement, despite rerouting flow at every time step. The LVI simulations have some drainage rearrangement, but very little and only in the headwaters. In contrast, in some of the TTLEM simulations, we observed that the network across the entire landscape changed, though generally in subtle ways. Thus, we hypothesized that drainage rearrangement was playing a part in the variation in times to steady state.

To test this hypothesis, we reran the initial set of TTLEM simulations, but this time we did not reroute the flow after every time step during the transient simulations, which is an available option within the TTLEM modeling environment. What we found is that there is much less variation in time to steady state with time step when comparing with the initial set of simulations (figure 3). The time series of all the steady-state metrics in the simulations without drainage rearrangement is very different

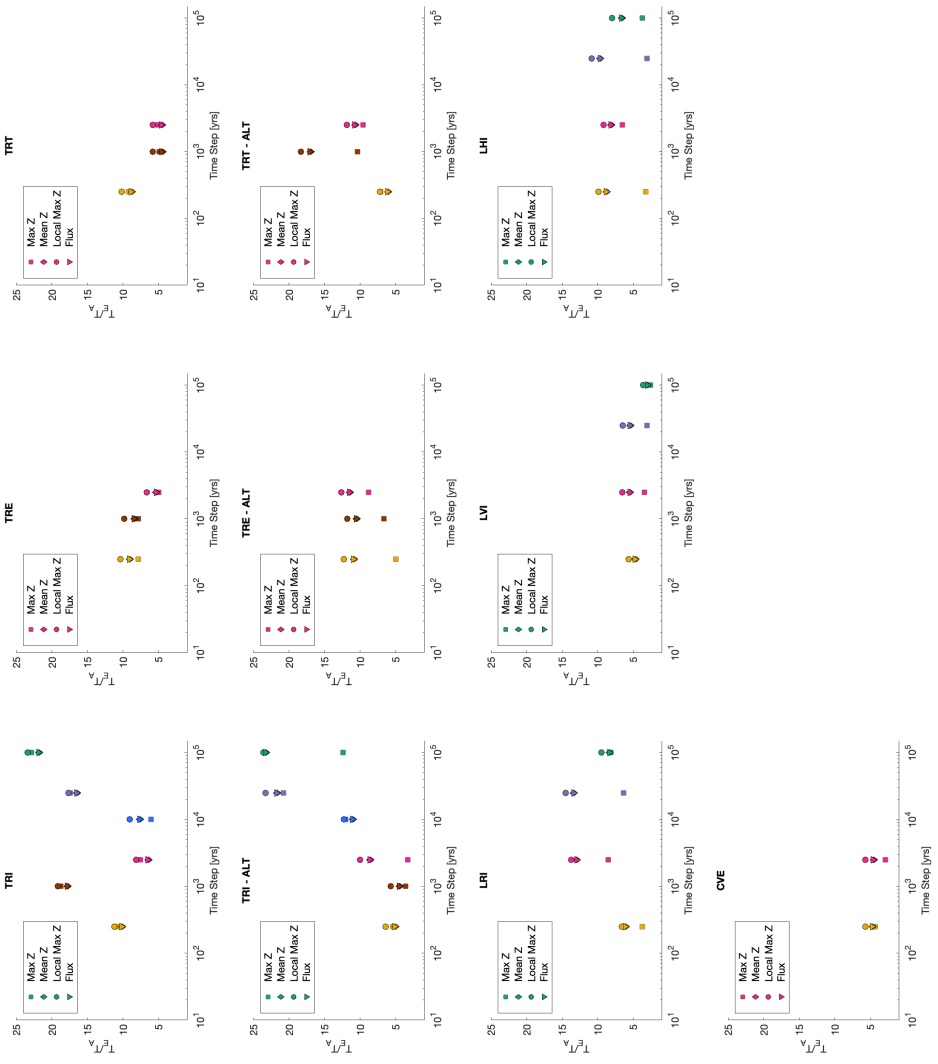

Figure 2. Ratio of the modeled to analytically predicted time to steady state as a function of time step for all of the modeling scenarios. The second row of results indicates the set of TTLEM simulations that used a different network for the initial conditions. Other than this change, everything was the same between TTLEM and TTLEM-ALT. Note that the extent of the x and y axes is the same in all of the subplots.

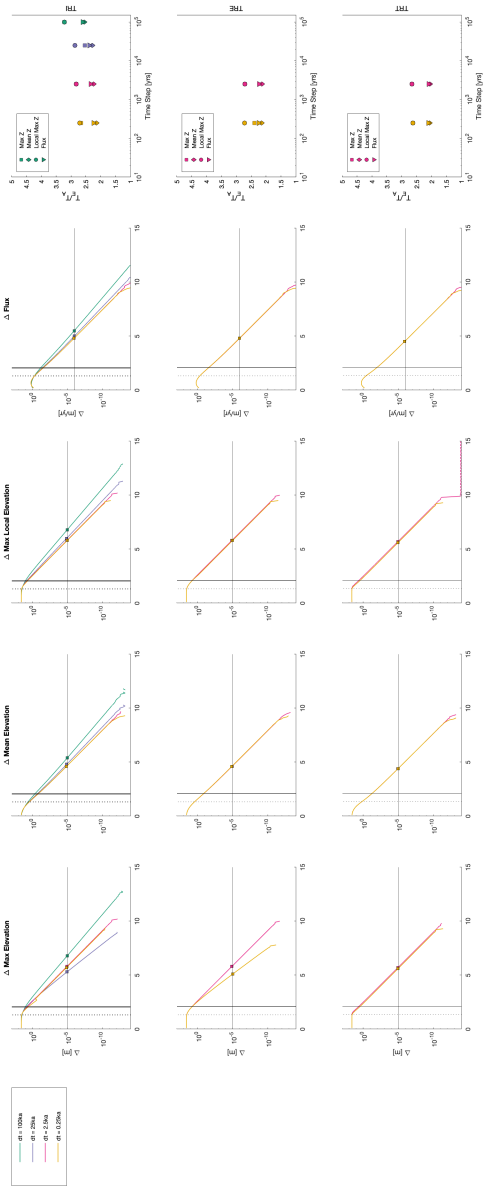

Figure 3. This figure is similar to Figures 1 and 2 except we only show TTLEM model results, and we did not reroute the flow after every time step. In other words, there was no drainage rearrangement in these simulations. Note the x axis in the first four columns is time in millions of years. The extent of the x and y axes in all of the time series is the same. The extent of the x and y axes

from the TTLEM simulations with drainage rearrangement. With a fixed network, all of the metrics remain nearly steady in the initial response, and then they monotonically decline.

7 Implications and Conclusions

At a minimum, the results of our experiments highlight that when simulating landscape evolution scenarios and considering topographic steady state—and especially time to steady state—it is critical to both report the metric being used and the threshold value for that metric to assess steady state. Generally, the strictly topographic metrics, i.e., those only tracking mean and maximum elevations, behaved similarly in the sense that a single threshold value can be used to estimate time to steady state within a specific simulation (e.g., figures 1 & 2). The flux-based metric also behaved similarly among simulations, although it required a lower threshold value to yield a comparable estimate.

Given the variability in T_E with respect to T_A from our experiments, a deeper question, regardless of exactly how steady state is assessed, is whether response times as interpreted from 2D landscape evolution models are meaningful or reliable. At first glance, the combination of T_E being consistently greater than T_A but by inconsistent magnitudes for a given identical set of conditions (e.g., uplift rate change, erosional efficiency, algorithm, grid type, and dt), would understandably give one reason to question the utility of response times from 2D landscape evolution models. An important related question, though, is the extent to which we expect the conditions assumed in calculating analytical response times T_A to be met in real landscapes, i.e., is T_A a fair or reasonable benchmark? Implicit in the calculation of T_A is an assumption of static stream length and drainage area during response to a change in either K or U (e.g., Whipple, 2001; Goren, 2016). Further, T_A reduces the network into 1-D, and the network structure provides a more complex transient response than predicted by 1-D models Li et al. (2018).

Comparing our experiments where flow routing is recomputed at every time step (figure 1) with those where the drainage network is fixed (figure 3) suggests that small perturbations in drainage network structure (e.g., single pixel to pixel changes in divide location or along the course of individual drainages) likely cause the longer response time compared to the predictions of T_A. Recent work highlighting that divide migration and drainage network instability may be more the norm (e.g. Willett et al., 2014; Whipple et al., 2017; Beeson et al., 2017; Forte and Whipple, 2018; Val et al., 2022), complicates the assumption of a static drainage network implied by calculations of T_A. Importantly, the majority of prior results arguing for pervasive drainage network reorganization consider scenarios with spatial gradients in either K or U, which our simple experiments do not include. It is possible that response times from 2D simulations driven by spatial gradients in environmental drivers and which generally induce greater amounts of network reorganization, like those considered for divide migration by Whipple et al. (2017) or Lyons et al. (2020), may be less sensitive to the initial conditions and small perturbations in the network than our simulations here. However, testing this is beyond the scope of this short communication.

In summary, if we are primarily concerned with the legitimacy of using results of landscape simulations to establish the time scale of processes or the evolution of specific landscapes, it is not immediately apparent that T_E as estimated from 2D numerical simulations is any more or less grounded in reality than T_A, but the variability of T_E with respect to T_A is especially problematic. Based on our experiments and the above, we provide a set of recommendations for considering steady state

and response times from 2D simulations. First and foremost, it is critical to remain mindful of the importance of the initial conditions (e.g., the random noise grid, or estimates of paleotopography) in dictating landscape evolution (e.g., Willgoose et al., 1991; Perron and Fagherazzi, 2012; Ferrier et al., 2013; Han et al., 2014; Ward and Galewsky, 2014) and to treat properties related to response times as more stochastic. Thus, one potentially useful approach is to consider T_A as a minimum response time. Ranges of more reasonable response times, incorporating some stochastic degree of minor drainage reorganization, can be estimated from multiple 2D simulations with different initial topographic conditions (i.e., random noise) for a given fixed set of other environmental factors. Also, our results highlight that choice of grid is meaningful in terms of reliability of T_E, with either voronoi or hex grids more likely to produce T_E estimates that do not vary as much as a function of dt. Thus these grid types may be more suitable where reliability of response times is important or where simulations run with different dt might be compared. The absolute most conservative approach to our results is to largely ignore response times as derived from 2D landscape evolution models and instead focus on landscape forms, either during the transient response or at quasi steady state, or as a function of non-dimensional time within a simulation.

Code and data availability. CHILD is distributed from this repository: https://github.com/childmodel/child; accessed 1 May 2023. Landlab is distributed from this repository: https://github.com/landlab/landlab; accessed 1 May 2023. TTLEM is distributed from this repository: https://github.com/wschwanghart/topotoolbox; accessed 1 May 2023. The initial grids, input files, and code for creating the figures for this manuscript are available from this repository: https://github.com/nicgaspar/LEM_comparison.

Author contributions. NG initiated this study and ran all the CHILD simulations. KB ran all the Landlab simulations. AF ran all the TTLEM simulations and made figures for the manuscript. NG wrote the first draft of the manuscript. All authors contributed to the design and direction of the study, interpreting the results, and refining the manuscript.

Competing interests. The authors have no competing interests to declare.

Acknowledgements. We gratefully acknowledge funding from the Tulane Oliver Fund, NSF Awards OAC-1450338 (NMG), EAR-1349375 (NMG), and EAR-1725774 (KRB). We acknowledge contributions from Nathan Lyons in the initial stages of this project. Conversations with Kelin Whipple, Brian Yanites, and Leif Karlstrom encouraged us to pursue this work. CSDMS enabled this modeling study. We also acknowledge the impact of the global COVID-19 pandemic on this study. The first draft of this manuscript was written in January 2020, but the work was put aside for two years due to NMG being overwhelmed by the excess work and family burdens created during a pandemic.

References

Adams, B. A., Whipple, K. X., Forte, A. M., Heimsath, A. M., and Hodges, K. V.: Climate controls on erosion in tectonically active landscapes, Science Advances, 6, https://doi.org/10.1126/sciadv.aaz3166, 2020.

Anders, A. M., Roe, G. H., Montgomery, D. R., and Hallet, B.: Influence of precipitation phase on the form of mountain ranges, Geology, 36, 479, https://doi.org/10.1130/G24821A.1, 2008.

Armitage, J. J., Whittaker, A. C., Zakari, M., and Campforts, B.: Numerical modelling of landscape and sediment flux response to precipitation rate change, Earth Surface Dynamics, 6, 77–99, 2018.

Attal, M., Tucker, G., Whittaker, A. C., Cowie, P., and Roberts, G. P.: Modeling fluvial incision and transient landscape evolution: Influence of dynamic channel adjustment, Journal of Geophysical Research: Earth Surface, 113, 2008.

Attal, M., Cowie, P. A., Whittaker, A. C., Hobley, D., Tucker, G. E., and Roberts, G. P.: Testing fluvial erosion models using the transient response of bedrock rivers to tectonic forcing in the Apennines, Italy, Journal of Geophysical Research: Earth Surface, 116, https://doi.org/10.1029/2010JF001875, _eprint: https://onlinelibrary.wiley.com/doi/pdf/10.1029/2010JF001875, 2011.

Barnhart, K. R., Hutton, E. W. H., Tucker, G. E., Gasparini, N. M., Istanbulluoglu, E., Hobley, D. E. J., Lyons, N. J., Mouchene, M., Nudurupati, S. S., Adams, J. M., and Bandaragoda, C.: Short communication: Landlab v2.0: a software package for Earth surface dynamics, Earth Surface Dynamics, 8, 379–397, https://doi.org/10.5194/esurf-8-379-2020, 2020.

Beeson, H. W., McCoy, S. W., and Keen-Zebert, A.: Geometric disequilibrium of river basins produces long-lived transient landscapes, Earth and Planetary Science Letters, 475, 34–43, 2017.

Braun, J. and Deal, E.: Implicit algorithm for threshold Stream Power Incision Model, Journal of Geophysical Research: Earth Surface, p. e2023JF007140, 2023.

Braun, J. and Willett, S. D.: A very efficient 0(n), implicit and parallel method to solve the stream power equation governing fluvial incision and landscape evolution, Geomorphology, 180-181, 170–179, https://doi.org/10.1016/j.geomorph.2012.10.008, 2013.

Brocard, G. Y., Willenbring, J. K., Miller, T. E., and Scatena, F. N.: Relict landscape resistance to dissection by upstream migrating knickpoints, Journal of Geophysical Research: Earth Surface, 121, 1182–1203, 2016.

Campforts, B. and Govers, G.: Keeping the edge: A numerical method that avoids knickpoing smearing when solving the stream power law, Journal of Geophysical Research: Earth Surface, 120, 1189–1205, https://doi.org/10.1002/2014JF003376.Received, 2015.

Campforts, B., Schwanghart, W., and Govers, G.: Accurate simulation of transient landscape evolution by eliminating numerical diffusion: the TTLEM 1.0 model, Earth Surface Dynamics, 5, 47–66, https://doi.org/10.5194/esurf-5-47-2017, publisher: Copernicus GmbH, 2017.

Campforts, B., Shobe, C. M., Overeem, I., and Tucker, G. E.: The art of landslides: How stochastic mass wasting shapes topography and influences landscape dynamics, Journal of Geophysical Research: Earth Surface, 127, e2022JF006 745, 2022.

Castelltort, S. and Van Den Driessche, J.: How plausible are high-frequency sediment supply-driven cycles in the stratigraphic record?, Sedimentary geology, 157, 3–13, 2003.

Densmore, A. L.: Footwall topographic development during continental extension, Journal of Geophysical Research, 109, F03 001, https://doi.org/10.1029/2003JF000115, 2004.

Densmore, A. L., Allen, P. A., and Simpson, G.: Development and response of a coupled catchment fan system under changing tectonic and climatic forcing, Journal of Geophysical Research: Earth Surface, 112, 2007.

Ferrier, K. L., Huppert, K. L., and Perron, J. T.: Climatic control of bedrock river incision, Nature, 496, 206–209, 2013.

Forte, A. M. and Whipple, K. X.: Criteria and tools for determining drainage divide stability, Earth and Planetary Science Letters, 493, 102–117, https://doi.org/10.1016/j.epsl.2018.04.026, 2018.

Forzoni, A., Storms, J. E., Whittaker, A. C., and de Jager, G.: Delayed delivery from the sediment factory: Modeling the impact of catchment response time to tectonics on sediment flux and fluvio-deltaic stratigraphy, Earth Surface Processes and Landforms, 39, 689–704, 2014.

Gasparini, N. M., Tucker, G. E., and Bras, R. L.: Network-scale dynamics of grain-size sorting: Implications for downstream fining, stream profile concavity, and drainage basin morphology, Earth Surface Processes and Landforms, 29, 401–421, 2004.

Gasparini, N. M., Whipple, K. X., and Bras, R. L.: Predictions of steady state and transient landscape morphology using sediment-flux-dependent river incision models, Journal of Geophysical Research: Earth Surface, 112, https://doi.org/10.1029/2006JF000567, _eprint: https://onlinelibrary.wiley.com/doi/pdf/10.1029/2006JF000567, 2007.

Godard, V., Tucker, G. E., Burch Fisher, G., Burbank, D. W., and Bookhagen, B.: Frequency-dependent landscape response to climatic forcing, Geophysical Research Letters, 40, 859–863, 2013.

Goren, L.: A theoretical model for fluvial channel response time during time-dependent climatic and tectonic forcing and its inverse applications, Geophysical Research Letters, 43, https://doi.org/10.1002/2016GL070451, 2016.

Hack, J. T.: Studies of longitudinal stream profiles in Virginia and Maryland, vol. 294, US Government Printing Office, 1957.

Han, J., Gasparini, N. M., Johnson, J. P., and Murphy, B. P.: Modeling the influence of rainfall gradients on discharge, bedrock erodibility, and river profile evolution, with application to the Big Island, Hawai'i, Journal of Geophysical Research: Earth Surface, 119, 1418–1440, 2014.

Han, J., Gasparini, N. M., and Johnson, J. P. L.: Measuring the imprint of orographic rainfall gradients on the morphology of steady-state numerical fluvial landscapes: OROGRAPHIC RAINFALL AND STEADY-STATE FLUVIAL LANDSCAPES, Earth Surface Processes and Landforms, 40, 1334–1350, https://doi.org/10.1002/esp.3723, 2015.

Hilley, G., Strecker, M. R., and Ramos, V.: Growth and erosion of fold-and-thrust belts with an application to the Aconcagua fold-and-thrust belt, Argentina, Journal of Geophysical Research: Solid Earth, 109, 2004.

Hobley, D. E. J., Adams, J. M., Nudurupati, S. S., Hutton, E. W. H., Gasparini, N. M., Istanbulluoglu, E., and Tucker, G. E.: Creative computing with Landlab: an open-source toolkit for building, coupling, and exploring two-dimensional numerical models of Earth-surface dynamics, Earth Surface Dynamics, 5, 21–46, https://doi.org/10.5194/esurf-5-21-2017, 2017.

Howard, A. D.: A detachment-limited model of drainage basin evolution, Water Resources Research, 30, 2261–2285, https://doi.org/10.1029/94WR00757, _eprint: https://onlinelibrary.wiley.com/doi/pdf/10.1029/94WR00757, 1994.

Hurst, M. D., Grieve, S. W., Clubb, F. J., and Mudd, S. M.: Detection of channel-hillslope coupling along a tectonic gradient, Earth and Planetary Science Letters, 522, 30–39, https://doi.org/10.1016/j.epsl.2019.06.018, 2019.

Kirby, E. and Whipple, K. X.: Expression of active tectonics in erosional landscapes, Journal of Structural Geology, 44, 54–75, 2012.

Lague, D.: The stream power river incision model: evidence, theory and beyond, Earth Surface Processes and Landforms, 39, 38–61, https://doi.org/10.1002/esp.3462, 2014.

Li, Q., Gasparini, N. M., and Straub, K. M.: Some signals are not the same as they appear: How do erosional landscapes transform tectonic history into sediment flux records?, Geology, 46, 407–410, 2018.

Lyons, N. J., Val, P., Albert, J. S., Willenbring, J. K., and Gasparini, N. M.: Topographic controls on divide migration, stream capture, and diversification in riverine life, Earth Surface Dynamics, 8, 893–912, https://doi.org/10.5194/esurf-8-893-2020, 2020.

Mackey, B. H., Scheingross, J. S., Lamb, M. P., and Farley, K. A.: Knickpoint formation, rapid propagation, and landscape response following coastal cliff retreat at the last interglacial sea-level highstand: Kaua 'i, Hawai 'i, Bulletin, 126, 925–942, 2014.

Perron, J. T. and Fagherazzi, S.: The legacy of initial conditions in landscape evolution, Earth Surface Processes and Landforms, 37, 52–63, 2012.

Roe, G. H., Whipple, K. X., and Fletcher, J. K.: Feedbacks among climate, erosion, and tectonics in a critical wedge orogen, American Journal of Science, 308, 815–842, 2008.

Roering, J. J.: How well can hillslope evolution models "explain" topography? Simulating soil transport and production with high-resolution topographic data, GSA Bulletin, 120, 1248–1262, https://doi.org/10.1130/B26283.1, 2008.

Romans, B. W., Castelltort, S., Covault, J. A., Fildani, A., and Walsh, J.: Environmental signal propagation in sedimentary systems across timescales, Earth-Science Reviews, 153, 7–29, 2016.

Rosenbloom, N. and Anderson, R. S.: Hillslope and channel evolution in a marine terraced landscape, Santa Cruz, California, Journal of Geophysical Research, 99, 14 013–14 029, 1994.

Schwanghart, W. and Scherler, D.: Short Communication: TopoToolbox 2 - MATLAB based software for topographic analysis and modeling in Earth surface sciences, Earth Surface Dynamics, 2, 1–7, https://doi.org/10.5194/esurf-2-1-2014, 2014.

Shobe, C. M., Tucker, G. E., and Rossi, M. W.: Variable-Threshold Behavior in Rivers Arising From Hillslope-Derived Blocks, Journal of Geophysical Research: Earth Surface, 123, 1931–1957, https://doi.org/10.1029/2017JF004575, 2018.

Simpson, G. and Castelltort, S.: Model shows that rivers transmit high-frequency climate cycles to the sedimentary record, Geology, 40, 1131–1134, 2012.

Snyder, N. P., Whipple, K. X., Tucker, G. E., and Merrits, D. J.: Landscape response to tectonic forcing: Digital elevation model analysis of stream profiles in the Mendocino triple junction region, northern California, Geological Society of America Bulletin, 112, 1250–1263, 2000.

Stolar, D. B., Willett, S. D., and Roe, G. H.: Climatic and tectonic forcing of a critical orogen, in: Tectonics, Climate, and Landscape Evolution, Geological Society of America, https://doi.org/10.1130/2006.2398(14), 2006.

Straub, K. M., Duller, R. A., Foreman, B. Z., and Hajek, E. A.: Buffered, incomplete, and shredded: The challenges of reading an imperfect stratigraphic record, Journal of Geophysical Research: Earth Surface, 125, e2019JF005 079, 2020.

Tarboton, D. G.: A new method for the determination of flow directions and upslope areas in grid digital elevation models, Water Resources Research, 33, 309–319, https://doi.org/10.1029/96wr03137, 1997.

Tofelde, S., Bernhardt, A., Guerit, L., and Romans, B. W.: Times associated with source-to-sink propagation of environmental signals during landscape transience, Frontiers in Earth Science, 9, 628 315, 2021.

Tucker, G. and Whipple, K.: Topographic outcomes predicted by stream erosion models: Sensitivity analysis and intermodel comparison, Journal of Geophysical Research: Solid Earth, 107, ETG–1, 2002.

Tucker, G. E. and Bras, R. L.: Hillslope processes, drainage density, and landscape morphology, Water Resources Research, 34, 2751–2764, https://doi.org/10.1029/98WR01474, _eprint: https://onlinelibrary.wiley.com/doi/pdf/10.1029/98WR01474, 1998.

Tucker, G. E., Gasparini, N. M., Bras, R. L., and Lancaster, S. L.: A 3D Computer Simulation Model of Drainage Basin and Floodplain Evolution: Theory and Applications, Technical report prepared for U.S. Army Corps of Engineers Construction Engineering Research Laboratory, 1999.

Tucker, G. E., Lancaster, S. T., Gasparini, N. M., and Bras, R. L.: The channel-hillslope intergrated landscape development model (CHILD), in: Landscape erosion and evolution modeling, edited by Harmon, R. S. and Doe, W. W., pp. 349–388, Springer, New York, 2001a.

Tucker, G. E., Lancaster, S. T., Gasparini, N. M., Bras, R. L., and Rybarczyk, S. M.: An object-oriened framework for distributed hydrologic and geomorphic modeling using triangulated irregular networks, Computers & Geosciences, 27, 959–973, 2001b.

Tucker, G. E., Hutton, E. W. H., Piper, M. D., Campforts, B., Gan, T., Barnhart, K. R., Kettner, A. J., Overeem, I., Peckham, S. D., McCready, L., and Syvitski, J.: CSDMS: a community platform for numerical modeling of Earth surface processes, Geoscientific Model Development, 15, 1413–1439, https://doi.org/10.5194/gmd-15-1413-2022, 2022.

Val, P., Lyons, N. J., Gasparini, N., Willenbring, J. K., and Albert, J. S.: Landscape evolution as a diversification driver in freshwater fishes, Frontiers in Ecology and Evolution, 9, 788 328, 2022.

Ward, D. J. and Galewsky, J.: Exploring landscape sensitivity to the Pacific Trade Wind Inversion on the subsiding island of Hawaii, Journal of Geophysical Research: Earth Surface, 119, 2048–2069, 2014.

Whipple, K. X.: Fluvial landscape response time: How plausible is steady-state denudation?, American Journal of Science, 301, 313–325, 2001.

Whipple, K. X. and Meade, B.: Controls on the strength of coupling among climate, erosion, and deformation in two-sided, frictional orogenic wedges at steady state, Journal of Geophysical Research, 109, F01 011–F01 011, https://doi.org/10.1029/2003JF000019, 2004.

Whipple, K. X. and Meade, B.: Orogen response to changes in climatic and tectonic forcing, Earth and Planetary Science Letters, 243, 218–228, 2006.

Whipple, K. X. and Tucker, G. E.: Dynamics of the stream-power river incision model: Implications for height limits of mountain ranges, landscape response timescales, and research needs, Journal of Geophysical Research: Solid Earth, 104, 17 661–17 674, https://doi.org/10.1029/1999JB900120, _eprint: https://onlinelibrary.wiley.com/doi/pdf/10.1029/1999JB900120, 1999.

Whipple, K. X. and Tucker, G. E.: Implications of sediment-flux-dependent river incision models for landscape evolution, Journal of Geophysical Research: Solid Earth, 107, ETG 3–1–ETG 3–20, https://doi.org/10.1029/2000JB000044, _eprint: https://onlinelibrary.wiley.com/doi/pdf/10.1029/2000JB000044, 2002.

Whipple, K. X., Forte, A. M., DiBiase, R. A., Gasparini, N. M., and Ouimet, W. B.: Timescales of landscape response to divide migration and drainage capture: Implications for the role of divide mobility in landscape evolution, Journal of Geophysical Research: Earth Surface, https://doi.org/10.1002/2016JF003973, 2017.

Whittaker, A. C.: How do landscapes record tectonics and climate, Lithosphere, 4, 160–164, 2012.

Whittaker, A. C. and Boulton, S. J.: Tectonic and climatic controls on knickpoint retreat rates and landscape response times, Journal of Geophysical Research: Earth Surface, 117, 2012.

Willett, S. D. and Brandon, M. T.: On steady states in mountain belts, Geology, 30, 175–178, 2002.

Willett, S. D., McCoy, S. W., Perron, J. T., Goren, L., and Chen, C.-Y.: Dynamic reorganization of river basins, Science, 343, 1248 765–1248 765, https://doi.org/10.1126/science.1248765, 2014.

Willgoose, G., Bras, R. L., and Rodriguez-Iturbe, I.: A coupled channel network growth and hillslope evolution model: 1. Theory, Water Resources Research, 27, 1671–1684, https://doi.org/10.1029/91WR00935, _eprint: https://onlinelibrary.wiley.com/doi/pdf/10.1029/91WR00935, 1991.